R_b and R_c in the two-Higgs-doublet model with flavor-changing neutral currents

David Atwood

Theory Group, Southeastern Universities Research Association, Continuous Electron Beam Accelerator Facility,
Newport News, Virginia 23606

Laura Reina and Amarjit Soni

Physics Department, Brookhaven National Laboratory, Upton, New York 11973

(Received 6 March 1996)

A study of R_b and R_c is presented in the context of a two-Higgs-doublet model with flavor-changing scalar currents (FCSC's). Implications of the model for the ρ parameter and for $b \to s\gamma$ are also considered. The experimental data on R_b places stringent constraints on the model parameters that are difficult to reconcile with the constraints from $b \to s\gamma$ and ρ. If we treat the couplings of the model as purely phenomenological, then the model can still survive albeit in a rather narrow region of the parameter space. Noting that aspects of the experimental analysis for R_b and R_c may be of some concern, we also disregard R_b^{expt} and R_c^{expt} and give predictions for these using constraints from $b \to s\gamma$ and the ρ parameter only. We emphasize the theoretical and experimental advantages of the observable $R_{b+c} \equiv \Gamma(Z \to b\bar{b} \text{ or } c\bar{c})/\Gamma(Z \to \text{hadrons})$. We also stress the role of $R_l \equiv \Gamma(Z \to \text{hadrons})/\Gamma(Z \to l^+l^-)$ in testing the standard model despite its dependence on QCD corrections. Noting that in models with FCNC's the amplitude for $Z \to c\bar{c}$ receives a contribution which grows with m_t^2 the importance and uniqueness of precision $Z \to c\bar{c}$ measurements for constraining flavor-changing $t\bar{c}$ currents is underscored. [S0556-2821(96)04517-1]

PACS number(s): 11.30.Hv, 12.60.Fr, 14.65.Fy

I. INTRODUCTION AND SUMMARY

For the past several years precision studies at the CERN e^+e^- collider LEP have been providing important confirmation to various aspects of the standard model (SM) [1]. A notable exception that has emerged is the decay of $Z \to b\bar{b}$. It has long been recognized that the $Zb\bar{b}$ vertex is very sensitive to effects of virtual, heavy particles [2]. Consequently, a deviation from the prediction of the SM could prove to be a significant clue to *new physics*. It is, therefore, clearly important to study $Z \to b\bar{b}$ in extensions of the SM [3] and pursue the resulting implications. In this paper we study these decays in a class of two-Higgs-doublet models (2HDM's), called model III [4–10], which present a natural mechanism for flavor changing scalar currents (FCSC's).

Our focus is the branching ratio of $Z \to b\bar{b}$: i.e. [1],

$$R_b \equiv \frac{\Gamma(Z \to b\bar{b})}{\Gamma(Z \to \text{hadrons})}. \tag{1}$$

It is worth noting that, since R_b is a ratio between two hadronic rates, most of the electroweak (EW) oblique and QCD corrections cancel between numerator and denominator, making it a uniquely clean and sensitive test of the SM. Experiment finds [1]

$$R_b^{\text{expt}} = 0.2205 \pm 0.0016, \tag{2}$$

whereas the SM prediction is [1]

$$R_b^{\text{SM}} = 0.2156. \tag{3}$$

The difference, of about 3σ, is a possible indication of new physics. We note, in passing, that the related decay $Z \to c\bar{c}$ has also been measured, albeit with appreciably less precision [1]:

$$R_c^{\text{expt}} = 0.1543 \pm 0.0074. \tag{4}$$

The SM prediction, on the other hand, is [1]

$$R_c^{\text{SM}} = 0.1724. \tag{5}$$

Thus R_c^{expt} also appears not to be consistent with the SM although the deviation is milder (about 2.3σ). It is interesting to note that whereas R_b^{expt} is larger than R_b^{SM}, R_c^{expt} is less than the SM expectation. Note also that R_b^{expt} quoted above is obtained by holding R_c fixed to its SM value [1].

Our findings are that if we take R_b^{expt} at its face value then, while model III can accommodate R_b^{expt}, the model parameters get severely constrained. In particular, the resulting configuration of the model can only be reconciled with the constraints from the ρ parameter and $B(B \to X_s\gamma)$ in a very small region of the parameter space.

Several aspects of the R_b and R_c experimental analysis are, though, of concern. The results given above in Eqs. (2) and (4) include systematic errors and emerge from combining the numbers from the four LEP detectors [1]. Since some of the assumptions are common, treatment of the systematics can be problematic. Also the errors for R_b and R_c are correlated [1]. Indeed $R_b^{\text{expt}} + R_c^{\text{expt}}$ is consistent with the SM ac-

centuating the possibility that part of the effect may well result from misidentification of the flavors. In addition, the observable R_l,

$$R_l \equiv \frac{\Gamma(Z \to \text{hadrons})}{\Gamma(Z \to l^+ l^-)}, \tag{6}$$

which is measured much more precisely than R_b or R_c and can be predicted in the SM using $\alpha_s(M_Z)$ deduced from other methods (e.g., lattice and/or event shapes in e^+e^- annihilation), is found not to be inconsistent with the SM, at present.

In light of these reservations we also fix the parameter space by using only the ρ parameter and $B(B \to X_s \gamma)$ and predict R_b and R_c in model III. In particular, in this model, with constraints from the ρ parameter and $B(B \to X_s \gamma)$, we find that R_b cannot exceed R_b^{SM}. Thus, if the current trend in the experimental numbers (i.e., $R_b^{\text{expt}} > R_b^{\text{SM}}$) persists, this class of 2HDM's will be either entirely ruled out or require a significant alteration.

In passing we also suggest a new observable

$$R_{b+c} = \frac{\Gamma(Z \to b\bar{b} \text{ or } c\bar{c})}{\Gamma(Z \to \text{hadrons})}, \tag{7}$$

which is theoretically as clean as R_b and R_c, but has some experimental advantages. Noting its possible usefulness, we give the prediction for R_{b+c} in model III .

Finally, we stress the importance of precision determinations of $Z \to c\bar{c}$ (i.e., R_c). In type-III models its amplitude receives a contribution which grows with m_t^2. A precise determination of $Z \to c\bar{c}$, thus, constitutes a uniquely clean method for constraining the flavor-changing tc vertex, which is of crucial theoretical concern. Improvements in the experimental determination of $Z \to c\bar{c}$ are therefore very worthwhile.

II. TWO-HIGGS-DOUBLET MODEL WITH FLAVOR-CHANGING CURRENTS

A mild extension of the SM with one additional scalar SU(2) doublet opens up the possibility of FCSC's. For this reason, the 2HDM scalar potential and Yukawa Lagrangian are usually constrained by an *ad hoc* discrete symmetry, [11] whose only role is to protect the model from tree-level FCSC's. As a result one gets the so-called model I and model II, when up-type and down-type quarks are coupled to the same or to two different doublets, respectively [12]. In particular, it is to be stressed that from a purely phenomenological point of view, low energy experiments involving K^0-$\bar{K}^0$, B^0-$\bar{B}^0$ mixing, $K_L \to \mu\bar{\mu}$, etc., place very stringent constraints only on the existence of those tree-level flavor-changing transitions which directly involve the first family. Indeed, in view of the extraordinary mass scale of the top quark, it has been emphasized by many that anomalously large flavor-changing (FC) couplings involving the third family may exist [4–10,13]. Thus, following Cheng and Sher [4], perhaps a natural way to limit the strength of the FCSC's involving the first family is to assume that they are proportional to the

masses of the participating quarks. In this way, the FC couplings are automatically put in a hierarchical order and the third family may well then play an enhanced role.

For this type of 2HDM, the Yukawa Lagrangian for the quark fields can be taken to have the form [8,9]

$$\mathcal{L}_Y^{(\text{III})} = \eta_{ij}^U \bar{Q}_{i,L} \widetilde{\phi}_1 U_{j,R} + \eta_{ij}^D \bar{Q}_{i,L} \phi_1 D_{j,R} + \xi_{ij}^U \bar{Q}_{i,L} \widetilde{\phi}_2 U_{j,R}$$
$$+ \xi_{ij}^D \bar{Q}_{i,L} \phi_2 D_{j,R} + \text{H.c.}, \tag{8}$$

where ϕ_i, for $i = 1,2$, are the two scalar doublets of a 2HDM, while $\eta_{ij}^{U,D}$ and $\xi_{ij}^{U,D}$ are the nondiagonal coupling matrices. For convenience we can choose to express ϕ_1 and ϕ_2 in a suitable basis such that only the $\eta_{ij}^{U,D}$ couplings generate the fermion masses, i.e., such that

$$\langle \phi_1 \rangle = \begin{pmatrix} 0 \\ v/\sqrt{2} \end{pmatrix}, \quad \langle \phi_2 \rangle = 0 \tag{9}$$

The two doublets are in this case of the form

$$\phi_1 = \frac{1}{\sqrt{2}} \left\{ \begin{pmatrix} 0 \\ v + H^0 \end{pmatrix} + \begin{pmatrix} \sqrt{2}\chi^+ \\ i\chi^0 \end{pmatrix} \right\}, \quad \phi_2 = \frac{1}{\sqrt{2}} \begin{pmatrix} \sqrt{2}H^+ \\ H^1 + iH^2 \end{pmatrix}. \tag{10}$$

The scalar Lagrangian in the $(H^0, H^1, H^2, H^\pm)$ basis is such that [14,12]

(1) the doublet ϕ_1 corresponds to the scalar doublet of the SM and H^0 to the SM Higgs field (same couplings and no interactions with H^1 and H^2), (2) all the new scalar fields belong to the ϕ_2 doublet, and (3) both H^1 and H^2 do not have couplings to the gauge bosons of the form $H^{1,2}ZZ$ or $H^{1,2}W^+W^-$.

However, while $H^\pm$ is also the charged scalar mass eigenstate, (H^0, H^1, H^2) are not the neutral mass eigenstates. Let us denote by $(\bar{H}^0, h^0)$ and A^0 the two scalar plus one pseudoscalar neutral mass eigenstates. They are obtained from (H^0, H^1, H^2) as follows

$$\bar{H}^0 = [(H^0 - v)\cos\alpha + H^1 \sin\alpha],$$

$$h^0 = [-(H^0 - v)\sin\alpha + H^1 \cos\alpha], \tag{11}$$

$$A^0 = H^2,$$

where α is a mixing angle, such that, for $\alpha = 0$, (H^0, H^1, H^2) coincide with the mass eigenstates. We find it more convenient to express H^0, H^1, and H^2 as functions of the mass eigenstates: i.e.,

$$H^0 = (\bar{H}^0 \cos\alpha - h^0 \sin\alpha) + v,$$

$$H^1 = (h^0 \cos\alpha + \bar{H}^0 \sin\alpha), \tag{12}$$

$$H^2 = A^0.$$

In this way we may take advantage of the mentioned properties (1), (2), and (3), as far as the calculation of the contribution from new physics goes. In particular, only the ϕ_1 doublet and the η_{ij}^U and η_{ij}^D couplings are involved in the generation of the fermion masses, while ϕ_2 is responsible for the new couplings.

After the rotation that diagonalizes the mass matrix of the quark fields, the FC part of the Yukawa Lagrangian looks like

$$\mathcal{L}_{Y,FC}^{(III)} = \hat{\xi}_{ij}^U \overline{Q}_{i,L} \widetilde{\phi}_2 U_{j,R} + \hat{\xi}_{ij}^D \overline{Q}_{i,L} \phi_2 D_{j,R} + \text{H.c.}, \quad (13)$$

where $Q_{i,L}$, $U_{j,R}$, and $D_{j,R}$ denote now the quark mass eigenstates and $\hat{\xi}_{ij}^{U,D}$ are the rotated couplings, in general not diagonal. If we define $V_{L,R}^{U,D}$ to be the rotation matrices acting on the up- and down-type quarks, with left or right chirality, respectively, then the neutral FC couplings will be

$$\hat{\xi}_{\text{neutral}}^{U,D} = (V_L^{U,D})^{-1} \cdot \xi^{U,D} \cdot V_R^{U,D}. \quad (14)$$

On the other hand, for the charged FC couplings we will have

$$\hat{\xi}_{\text{charged}}^U = \hat{\xi}_{\text{neutral}}^U \cdot V_{\text{CKM}},$$

$$\hat{\xi}_{\text{charged}}^D = V_{\text{CKM}} \cdot \hat{\xi}_{\text{neutral}}^D, \quad (15)$$

where V_{CKM} denotes the Cabibbo-Kobayashi-Maskawa (CKM) matrix. To the extent that the definition of the $\xi_{ij}^{U,D}$ couplings is arbitrary, we can take the rotated couplings as the original ones. Thus, we will denote by $\xi_{ij}^{U,D}$ the new rotated couplings in Eq. (14), such that the charged couplings in Eqs. (15) look like $\xi^U \cdot V_{\text{CKM}}$ and $V_{\text{CKM}} \cdot \xi^D$.

We will assume that the $\xi_{ij}^{U,D}$ couplings are purely phenomenological parameters and compare the region of the parameter space that could accommodate R_b^{expt} with the constraints from other physical processes. For convenience, we parametrize the $\xi_{ij}^{U,D}$ couplings in such a way as to make the comparison with the other 2HDM's easier:

$$\xi_{ij}^{U,D} = \lambda_{ij} \frac{\sqrt{m_i m_j}}{v}. \quad (16)$$

This is very similar to what was proposed and used in Refs. [4,8–10], but we want now to allow the factors λ_{ij} to vary over a broad range, constrained by phenomenology only. In this way we may be able to see if the experiment data lead to some new patterns in the coupling behavior [15].

III. IMPLICATIONS FOR R_b AND R_c

Let us now focus on the calculation of R_b and R_c. The main task is to compute the corrections from new physics to the SM $Zq\overline{q}$ vertex, for $q = c,b$. Suppose the reference SM vertex for a $Z \to q\overline{q}$ process is

$$V_{q\overline{q}Z}^{\text{SM}} \equiv -i \frac{g_W}{c_W} \overline{q} \gamma_\mu \left[\Delta_{q,L}^{\text{SM}} \frac{(1-\gamma_5)}{2} + \Delta_{q,R}^{\text{SM}} \frac{(1+\gamma_5)}{2} \right] q Z^\mu, \quad (17)$$

where c_W is the cosine of the Weinberg angle and g_W is the weak gauge coupling. The presence of new interactions will then modify it into

$$V_{q\overline{q}Z} \equiv -i \frac{g_W}{c_W} \overline{q} \gamma_\mu \left[\Delta_{q,L} \frac{(1-\gamma_5)}{2} + \Delta_{q,R} \frac{(1+\gamma_5)}{2} \right] q Z^\mu, \quad (18)$$

where

$$\Delta_{q,L(R)} \equiv \Delta_{q,L(R)}^{\text{SM}} + \Delta_{q,L(R)}^{\text{new}} \quad (19)$$

is the sum of the original SM contribution plus the new one from ξ-type scalar couplings. In principle, both SM and model III radiative corrections to the $Zq\overline{q}$ vertex give origin to one additional form factor, proportional to $\sigma^{\mu\nu} q_\nu$ (the $\sigma^{\mu\nu} q_\nu \gamma_5$ form factor is absent because it would violate CP). This magnetic-moment-type form factor arises at one loop and should be considered as well. We have calculated it and verified that, as is the case in the SM, it is very small, at least three orders of magnitude smaller than the leading contributions to $\Delta_{q,L(R)}^{\text{new}}$. Therefore, we neglect its effect in the following discussion.

In view of the previous discussion and neglecting all finite quark mass effects ($m_q \sim 0$) [17], the generic expression for $\Gamma(Z \to q\overline{q})$, $q = b,c$, can then be written as

$$\Gamma(Z \to q\overline{q}) = \frac{N_c}{6} \frac{\hat{\alpha}}{\hat{s}_W^2 \hat{c}_W^2} M_Z [(\Delta_{q,L})^2 + (\Delta_{q,R})^2], \quad (20)$$

where all kinds of EW+QCD corrections have been reabsorbed in the redefinition of the QED fine-structure constant α, of c_W (s_W), and of the couplings $\Delta_{q,L(R)}$. Moreover, the $\Delta_{q,L(R)}$ couplings contain corrections induced by the new FC scalar couplings.

In order to compute the corrections to R_q from new physics, such as due to the scalar fields of model III, we observe that, since R_q is the ratio between two hadronic widths, most EW oblique and QCD corrections cancel, in the massless limit, between the numerator and the denominator. The remaining ones are absorbed in the definition of the renormalized couplings $\hat{\alpha}$ and $\hat{s}_W$ ($\hat{c}_W$), up to terms of higher order in the electroweak corrections [2,18,19]. As a consequence, the $\Delta_{q,L(R)}$ couplings will be as in Eq. (18), with $\Delta_{q,L(R)}^{\text{SM}}$ given by the tree-level SM couplings expressed in terms of the renormalized couplings $\hat{\alpha}$ and $\hat{s}_W$ ($\hat{c}_W$). This feature makes the study of R_b and R_c particularly interesting, because the new FC contributions may be easily disentangled in the $Zq\overline{q}$-vertex corrections. In fact, the presence of new scalar-fermion couplings will affect the W and Z renormalized propagators too, giving stringent constraints especially from the corrections to the ρ parameter. However, this is not rel-
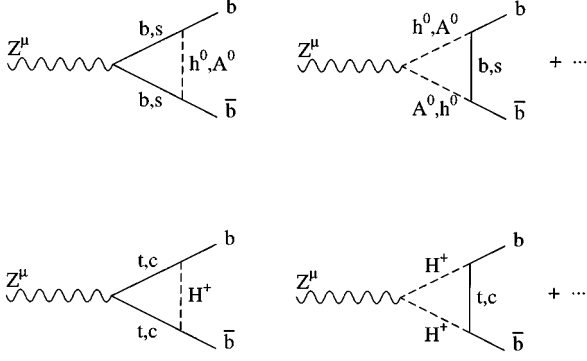
FIG. 1. Typical corrections to the $Zb\bar{b}$ vertex due to both charged and neutral scalar and pseudoscalar, in model III.

evant for the specific calculation of R_b and will be discussed in later segments of this paper.

In light of the preceding remarks, we can express R_b and R_c in terms of R_b^{SM} and R_c^{SM} as

$$R_q = R_q^{SM} \frac{1 + \delta_q}{[1 + R_b^{SM}\delta_b + R_c^{SM}\delta_c]}, \qquad (21)$$

where

$$\delta_q = 2 \frac{\Delta_{qL}^{SM}\Delta_{qL}^{new} + \Delta_{qR}^{SM}\Delta_{qR}^{new}}{(\Delta_{qL}^{SM})^2 + (\Delta_{qR}^{SM})^2} \qquad (22)$$

for $q = b,c$. In Eq. (21), terms of $O((\Delta_{qL(R)}^{new})^2)$ have been neglected and the numerical analysis confirms the validity of this approximation.

In particular, we will have to compute $\Delta_{b,L(R)}^{new}$ and $\Delta_{c,L(R)}^{new}$ in our model. In Fig. 1 we show a sample of the Feynman diagrams which correspond to the corrections to the $Zb\bar{b}$ vertex, due to both charged and neutral scalars or pseudoscalars. The $Zc\bar{c}$ case is strictly analogous, up to modifications of the external and internal quark states. In our calculation, we will assume that the FC couplings involving the first generation are negligible and we will consider all the other possible contributions from the new ξ-type vertices, containing both flavor-changing and flavor-diagonal terms [see Eqs. (13)–(16)]. Moreover, we will focus mainly on fixing the model parameters by using R_b^{expt} and then see what the implications for R_c are.

We examined various possible scenarios, varying the scalar masses (M_H, M_h, M_A, and M_c), the mixing angle (α), and the ξ couplings. The striking result emerging from this analysis is that, in spite of the arbitrariness of the new FC couplings, there exists only a very small window in which the corrections from this new physics enhance R_b to make it compatible with the experimental indications. We find that, in order to have maximum enhancement, the following requirements are crucial:

(1) Very large $h^0 b\bar{b}$ and $A^0 b\bar{b}$ couplings, obtained when

$$\xi_{bb}^D = \lambda_{bb} \frac{m_b}{v} \quad \text{and} \quad \lambda_{bb} \gg 1. \qquad (23)$$

(2) The phase $\alpha = 0$.

(3) Light and approximately equal neutral scalar and pseudoscalar masses:

$$50 \text{ GeV} \lesssim M_h \sim M_A \lesssim 70 \text{ GeV}, \qquad (24)$$

i.e., at the edge of the allowed experimental lower bound for M_h and M_A [20].

(4) Much heavier charged scalar masses, i.e., $M_c \gg M_h, M_A$. Lighter charged masses require even more demanding bounds on the previous parameters.

This set of parameters strictly mimics what was already found in the context of model II, i.e., without tree-level FCNC's. The pattern of cancellation between neutral and charged contributions is still valid in model III as well. The charged contribution to $\Delta_{b,L(R)}^{new}$ is negative and tends to reduce R_b, while the neutral one, for light scalar masses ($M_{h,A} < 100$ GeV), is positive and tends to enhance R_b. With an assumption like the one in Eq. (16), the neutral scalar and pseudoscalar vertex corrections are suppressed due to their small couplings to the b quark, unless $\lambda_{bb} \gg 1$. Thus, in order to enforce the cancellation, we have to enhance these couplings as in Eq. (23) as well as to demand that the charged scalar be much heavier than the neutral scalar and pseudoscalar.

Indeed our model can be compared to model II when the phase $\alpha = 0$ (as also required by R_b^{expt}), and the FC couplings are set to zero, i.e., $\xi_{sb}^D = 0$ and $\xi_{ct}^U = 0$. Then, the crucial difference between the two models is that model III, unlike model II, does not provide any relation between ξ^U- and ξ^D-type couplings. In model II ξ_{bb}^D is inversely proportional to ξ_{tt}^U and we would have at the same time a very enhanced ξ^D-type coupling and a very suppressed ξ^U-type one. As we will see, the relation between ξ^U- and ξ^D-type couplings will be extremely important in the study of $B(B \to X_s \gamma)$. Therefore in our analysis of R_b within model III we want to examine a few of the possible different scenarios.

To compare model III with model II (for vanishing FC couplings) we will consider the following two prototype cases.

Case 1:

$$\xi_{bb}^D = \lambda_{bb} \frac{m_b}{v} \quad \text{for} \quad \lambda_{bb} \gg 1, \qquad \xi_{tt}^U = \lambda_{tt} \frac{m_t}{v} \quad \text{for} \quad \lambda_{tt} \simeq 1. \qquad (25)$$

Case 2:

$$\xi_{bb}^D = \lambda_{bb} \frac{m_b}{v} \quad \text{for} \quad \lambda_{bb} \gg 1, \qquad \xi_{tt}^U = \lambda_{tt} \frac{m_t}{v} \quad \text{for} \quad \lambda_{tt} \simeq \frac{1}{\lambda_{bb}}. \qquad (26)$$

In principle both cases are possible if we assume the λ_{ij} parameters of Eq. (16) to be arbitrary and constrained only by experiments. In particular case 2 mimics model II and that will be useful for comparison. In both cases we can get R_b

within 2σ of R_b^{expt} (where $R_b^{\text{expt}} = 0.2219 \pm 0.0017$ [21]) when, in case 1, $\lambda_{bb} \gtrsim 65$ and $M_c \gtrsim 350$ GeV and, in case 2, $\lambda_{bb} \gtrsim 55$ and $M_c \gtrsim 150$ GeV. M_c can be lowered somewhat, provided we increase λ_{bb} even further and vice versa. In case 1 we have to impose some more demanding bounds because the charged contribution is not suppressed by the couplings but only by M_c. On the other hand, in case 2 we are able to confirm the results obtained for model II in Refs. [18,19]. No major dependence on ξ_{cc}^U and ξ_{ss}^D is observed in either case.

We want now to switch on the FC couplings ξ_{sb}^D and ξ_{ct}^U and analyze the differences. We note that, as far as R_b is concerned, ξ_{ct}^U plays a role only in the charged contribution to $\Delta_{b,L(R)}^{\text{new}}$ and, since this contribution is negative, we do not want to enhance it. On the other hand, ξ_{sb}^D affects both the neutral and the charged vertex diagram; thus, in principle, it could play some role. In particular we observe the following.

In case 1, any suppression of ξ_{ct}^U is irrelevant. On the other hand any enhancement of ξ_{sb}^D helps to get a little closer to the experimental values of R_b. A good choice of parameters is

$$\lambda_{bb} \gtrsim 60, \quad \lambda_{sb} \gtrsim 10, \quad \lambda_{tt} \sim \lambda_{ct} \sim 1, \text{ and } M_c \gtrsim 350 \text{ GeV.} \tag{27}$$

In case 2, ξ_{ct}^U has to be suppressed and ξ_{sb}^D enhanced. A good agreement with R_b^{expt} is obtained for

$$\lambda_{bb} \gtrsim 55, \quad \lambda_{sb} \gtrsim 10, \quad \lambda_{tt} \sim \lambda_{ct} \sim \frac{1}{\lambda_{bb}}, \text{ and } M_c \gtrsim 150 \text{ GeV.} \tag{28}$$

We observe that as far as R_b is concerned the two scenarios are not too different. Case 2 has the nice feature of imposing a much weaker lower bound on M_c. In both of them R_c turns out to be also compatible with R_c^{expt} at the 2σ level. A more precise determination of R_c^{expt} would play an important role at this level. In Sec. IV and V we will see which of these scenarios can survive the additional constraints imposed by ρ and $B(B \to X_s \gamma)$.

IV. ρ-PARAMETER CONSTRAINTS ON MODEL III

The relation between M_W and M_Z is modified by the presence of new physics and the deviation from the SM prediction is usually described by introducing the parameter ρ_0 [20,22], defined as

$$\rho_0 = \frac{M_W^2}{\rho M_Z^2 \cos^2 \theta_W}, \tag{29}$$

where the ρ parameter reabsorbs all the SM corrections to the gauge boson self-energies. We recall that the most important SM corrections at the one-loop level are induced by the top quark [19,22]:

$$\rho_{\text{top}} \simeq \frac{3 G_F m_t^2}{8\sqrt{2}\pi^2}. \tag{30}$$

Within the SM with only one scalar SU(2) doublet $\rho_0^{\text{tree}} = 1$. In the presence of new physics we have

$$\rho_0 = 1 + \Delta\rho_0^{\text{new}}, \tag{31}$$

where $\Delta\rho_0^{\text{new}}$ can be written in terms of the new contributions to the W and Z self-energies as

$$\Delta\rho_0^{\text{new}} = \frac{A_{WW}^{\text{new}}(0)}{M_W^2} - \frac{A_{ZZ}^{\text{new}}(0)}{M_Z^2}. \tag{32}$$

Using the general analytical expressions in Ref. [23], and adapting the discussion to model III (making use of the Feynman rules given in Appendix A), we find that

$$\Delta\rho_0^{\text{new}} \simeq \frac{G_F}{8\sqrt{2}\pi^2} [\sin^2\alpha G(M_c, M_A, M_H) + \cos^2\alpha G(M_c, M_A, M_h)], \tag{33}$$

where all the terms of order $(M_{W,Z}^2/M_c^2)$ have been neglected and we define

$$\begin{aligned} G(M_c, M_A, M_{H,h}) = M_c^2 &- \frac{M_c^2 M_A^2}{M_c^2 - M_A^2} \ln\frac{M_c^2}{M_A^2} \\ &- \frac{M_c^2 M_{H,h}^2}{M_c^2 - M_{H,h}^2} \ln\frac{M_c^2}{M_{H,h}^2} \\ &+ \frac{M_A^2 M_{H,h}^2}{M_A^2 - M_{H,h}^2} \ln\frac{M_A^2}{M_{H,h}^2}. \end{aligned} \tag{34}$$

The determination of m_t from Fermilab [24] allows us to distinguish between ρ_0 and $\rho \simeq 1 + \rho_{\text{top}}$. From the recent global fits of the electroweak data, which include the input for m_t from Ref. [24] and the new results on R_b, ρ_0 turns out to be very close to unity. For $R_b = R_b^{\text{expt}}$ as in Eq. (2) and $m_t = (174 \pm 16)$ GeV, Ref. [22] quotes

$$\rho_0 = 1.0004 \pm 0.0018 \pm 0.0018. \tag{35}$$

This result clearly imposes stringent limits on the parameters of any extended model. In particular, if we refer to Sec. III and evaluate $\Delta\rho_0^{\text{new}}$ for the set of parameters which was found to give an enhanced value of R_b [see Eqs. (23) and (24) in particular], we find that

$$\Delta\rho^{\text{new}} \simeq \frac{G_F}{8\sqrt{2}\pi^2} M_c^2, \tag{36}$$

where the neglected terms are suppressed as $(M_{h,A}^2/M_c^2)$ or $(M_{W,Z}^2/M_c^2)$. We observe that, for $\alpha = 0$, the contributions of the ϕ_1 and ϕ_2 doublets are completely decoupled and the new physics contributions come from the ϕ_2 doublet only. The ϕ_1 doublet can indeed be identified with the usual SM

Higgs doublet and its contribution to ρ_0 is already included in the SM value of ρ. Using Eq. (36), Eqs. (31) and (35) lead to the following upper bound on the charged scalar mass:

$$M_c \lesssim 200 \text{ GeV}, \qquad (37)$$

when M_h and M_A satisfy Eq. (24) as required by R_b^{expt}. The upper bound (37) for M_c is still compatible with case 2 [see Eq. (28)]. However, to retain R_b within 2σ of the experimental value in case 1 would require more demanding bounds on the $\xi_{ij}^{U,D}$ coupling than in Eqs. (27), since the latter were obtained with $M_c \gtrsim 350$ GeV and since, also, we cannot reduce the neutral scalar masses below their experimental bounds.

V. IMPLICATIONS OF $b \to s\gamma$

The real distinction between the previous two scenarios of model III and the other 2HDM's (model I and model II) is made by the experimental constraint on $B(B \to X_s\gamma)$ [25]:

$$B(B \to X_s\gamma) = (2.32 \pm 0.51 \pm 0.29 \pm 0.32) \times 10^{-4}, \quad (38)$$

where the first error is statistical and the latter two are systematic errors.

We will not consider model I, because it cannot produce an acceptable answer for R_b, since the fermion-scalar couplings in this model are either all simultaneously enhanced or simultaneously suppressed. Thus a disparity between neutral and charged scalar vertex corrections can never be realized in model I. Instead, let us focus on model II and model III. It is interesting to compare what ''the enhancement of the ξ_{bb}^D coupling'' means in these two models. We then immediately realize that in model III this implies a new large contribution from the neutral scalar and pseudoscalar penguin diagrams and a possible big enhancement of the charged scalar penguin diagram, due to the link between neutral and charged coupling via Eq. (15).

To calculate the contribution of h_0, A_0, and $H^\pm$ to the $B(B \to X_s\gamma)$, we work in the effective Hamiltonian formalism, thereby including also QCD corrections at the leading order [26]. Because of the presence of new effective interactions, we need to modify both the basis of local operators in the effective Hamiltonian and the initial conditions for the evolution of the Wilson coefficients. This is a well-known procedure for calculating the effect of heavy new degrees of freedom which do not appear in the evolution of the coefficients at low energy, but only in their initial conditions at an initial scale roughly set at $\mu \sim M_W$. We refer to the literature for all the necessary technical details [27–29].

In particular, when we include the new heavy degrees of freedom (h_0, A_0, and $H^\pm$), there are two main changes that we need to consider. First, there are now two QED magnetic-type operators with opposite chirality, which we denote by $Q_7^{(R,L)}$ and write as [30]

$$Q_7^{(R,L)} = \frac{e}{8\pi^2} m_b \bar{s} \sigma^{\mu\nu} (1 \pm \gamma_5) b F_{\mu\nu}. \qquad (39)$$

We recall that in the SM as well as in model II the absence of $Q_7^{(L)}$ is a consequence of assuming $m_s/m_b \sim 0$. In model III,

we do not want to make any *a priori* assumption on the ξ couplings, because of their arbitrariness, and therefore both $Q_7^{(R)}$ and $Q_7^{(L)}$ can contribute to the $b \to s\gamma$ decay. The rate $\Gamma(b \to s\gamma)$ will be proportional to the sum of the modulus square of their coefficients at a scale $\mu \sim m_b$: i.e.,

$$\Gamma(b \to s\gamma) \sim |C_7^{(R)}(m_b)|^2 + |C_7^{(L)}(m_b)|^2. \qquad (40)$$

We observe that, because of their opposite chirality, the two operators $Q_7^{(R,L)}$ do not mix under QCD corrections and, in a first approximation, their evolution with the scale μ can be taken to be the same as in the SM (for $Q_7^{(R)}$) and equal for both of them. In so doing, we neglect those operators whose effect is subleading either because of their chiral structure or because of the heavy mass of the scalar boson which generates them.

The second change concerns the initial conditions for the Wilson coefficients at a scale $\mu \sim M_W$. $C_7^{(R,L)}(m_b)$ depend in general on many initial conditions. However, for the same reasons as explained before, the most relevant new contributions, due both to neutral and charged scalar fields, mainly affect $C_7^{(R,L)}(M_W)$. In the following we will discuss the results of our numerical evaluation of both neutral and charged contributions and their impact on the decay rate for $b \to s\gamma$. In particular, we will focus on the rate normalized to the QCD corrected semileptonic rate, i.e., on the ratio

$$R = \frac{\Gamma(B \to X_s\gamma)}{\Gamma(B \to X_c e\bar{\nu}_e)} \sim \frac{\Gamma(b \to s\gamma)}{\Gamma(b \to ce\bar{\nu}_e)}$$

$$= \frac{6\alpha}{\pi f(m_c/m_b)} F[|C_7^{(R)}(m_b)|^2 + |C_7^{(L)}(m_b)|^2], \quad (41)$$

where $f(m_c/m_b)$ is the phase-space factor for the semileptonic decay and F takes into account some $O(\alpha_s)$ corrections to both $B \to X_c e\bar{\nu}_e$ and $B \to X_s\gamma$ decays (see Ref. [31] for further comments). We also neglect possible deviations from the spectator model prediction of $\Gamma(B \to X_s\gamma)$ and $\Gamma(B \to X_c e\bar{\nu}_e)$. From Eq. (41) a convenient theoretical prediction for $B(B \to X_s\gamma)$ can be extracted to be compared with the experimental result.

As far as the new FC contributions from neutral scalars and pseudoscalars go, they are peculiar to model III, because they contain FC couplings. Were it not for the enhancement of ξ_{bb}^D they would be completely negligible. When $\xi_{bb}^D \gtrsim 60 m_b/v$, however, the h_0 and A_0 penguin diagrams give a sizable contribution, amounting to an about 30% correction to the SM amplitude. This is still within the range allowed by the experiments and constitutes a first non-negligible point of difference with respect to model II.

However, the most striking effect emerges when we consider the charged scalar penguin. Let us focus separately on $C_7^{(R)}(M_W)$ and $C_7^{(L)}(M_W)$ and try to make a direct comparison with model II. We recall that the charged couplings for model II are given by

$$\mathcal{L}_Y^{(II)} = \sqrt{\frac{4G_F}{\sqrt{2}}} H^+ \left[\tan\beta \, \bar{U}_L V_{CKM} M_D D_R \right.$$

$$\left. + \frac{1}{\tan\beta} \bar{U}_R M_U V_{CKM} D_L \right] + \text{H.c.}, \qquad (42)$$

where M_U and M_D are the diagonal mass matrices for U-type and D-type quarks, respectively, and $\tan\beta = v_2/v_1$ is the ratio between the vacuum expectation values of the two scalar doublets. The analogous couplings for model III are expressed by Eqs. (13) and (15).

Both in model II and in model III, the new contributions to $C_7^{(R)}(M_W)$ happens to be multiplied by two products of Yukawa couplings, which we will denote by $(\xi_{st}^{U*}\xi_{tb}^U)_{ch}$ and $(\xi_{st}^{U*}\xi_{tb}^D)_{ch}$. Using Eq. (42), we derive that, in model II, these products of Yukawa couplings are given by

$$(\xi_{st}^{U*}\xi_{tb}^U)_{ch}^{(II)} = \frac{4G_F}{\sqrt{2}} V_{ts}^* V_{tb} m_t^2 \frac{1}{\tan\beta^2},$$

$$(\xi_{st}^{U*}\xi_{tb}^D)_{ch}^{(II)} = \frac{4G_F}{\sqrt{2}} V_{ts}^* V_{tb} m_t m_b. \qquad (43)$$

On the other hand, in model III, using Eqs. (13) and (15) they can be written as

$$(\xi_{st}^{U*}\xi_{tb}^U)_{ch}^{(III)} = V_{ts}^* V_{tb} \left(\xi_{tt}^U + \xi_{ct}^U \frac{V_{cs}^*}{V_{ts}^*} \right) \left(\xi_{tt}^U + \xi_{tc}^U \frac{V_{cb}}{V_{tb}} \right),$$

$$(\xi_{st}^{U*}\xi_{tb}^D)_{ch}^{(III)} = V_{ts}^* V_{tb} \left(\xi_{tt}^U + \xi_{ct}^U \frac{V_{cs}^*}{V_{ts}^*} \right) \left(\xi_{bb}^D + \frac{V_{ts}}{V_{tb}} \xi_{sb}^D \right). \qquad (44)$$

In order to compare the two models, let us use the parametrization introduced in Eq. (16) and let us set all the FC couplings in model III to zero, namely, $\xi_{ct}^U = 0$ and $\xi_{sb}^D = 0$. Then, the couplings in Eq. (44) reduce to the form

$$(\xi_{st}^{U*}\xi_{tb}^U)_{ch}^{(III)} = V_{ts}^* V_{tb} (\xi_{tt}^U)^2 = \frac{4G_F}{\sqrt{2}} V_{ts}^* V_{tb} (\lambda_{tt})^2 m_t^2,$$

$$(\xi_{st}^{U*}\xi_{tb}^D)_{ch}^{(III)} = V_{ts}^* V_{tb} \xi_{tt}^U \xi_{bb}^D = \frac{4G_F}{\sqrt{2}} V_{ts}^* V_{tb} (\lambda_{tt}\lambda_{bb}) m_t m_b. \qquad (45)$$

From Eqs. (43) and (45), the different behavior of model II and model III with respect to an enhancement of the ξ_{bb}^D-like coupling should be clear. The following correspondence holds:

$$\begin{array}{ccccc} & & \text{model II} & & \text{model III} \\ (\xi_{st}^{U*}\xi_{tb}^U)_{ch} & : & \dfrac{1}{\tan\beta^2} & \rightarrow & \lambda_{tt}^2 \\[2mm] (\xi_{st}^{U*}\xi_{tb}^D)_{ch} & : & 1 & \rightarrow & \lambda_{tt}\lambda_{bb} . \end{array} \qquad (46)$$

In model II, the enhancement of ξ_{bb}^D corresponds to the choice of large value for $\tan\beta$, i.e., to a suppression of the

$(\xi_{st}^{U*}\xi_{tb}^U)_{ch}$ coupling with respect to the $(\xi_{st}^{U*}\xi_{tb}^D)_{ch}$ one, which stays the same, i.e., pretty small. In model III, the result depends on the assumption we make on the λ_{tt}. Moreover, there will be some effect due to the FC couplings.

Finally, let us now consider $C_7^{(L)}(M_W)$. This coefficient is special to model III since it is normally neglected in model II in the limit $m_s/m_b \sim 0$. It turns out to be proportional to the other two possible combinations of Yukawa couplings, i.e.,

$$(\xi_{st}^{D*}\xi_{tb}^U)_{ch}^{(III)} = V_{ts}^* V_{tb} \left(\frac{V_{tb}}{V_{ts}^*} \xi_{bs}^D + \xi_{ss}^D \right) \left(\xi_{tt}^U + \xi_{tc}^U \frac{V_{cb}}{V_{tb}} \right),$$

$$(\xi_{st}^{D*}\xi_{tb}^D)_{ch}^{(III)} = V_{ts}^* V_{tb} \left(\frac{V_{tb}}{V_{ts}^*} \xi_{bs}^D + \xi_{ss}^D \right) \left(\xi_{bb}^D + \frac{V_{ts}}{V_{tb}} \xi_{sb}^D \right), \qquad (47)$$

and constitutes a relevant extra contribution to $B(B \rightarrow X_s \gamma)$, to the extent that the FC couplings, namely, ξ_{bs}^D and/or ξ_{ct}^U, are not negligible.

In view of the previous discussion, in our numerical analysis we have considered the two scenarios denoted as case 1 and case 2 in Sec. III. We find the following.

In case 1, since λ_{bb} is greatly enhanced and λ_{tt} is not suppressed, the net result is that the charged scalar penguin diagram is greatly enhanced even with $\xi_{ct}^U = 0$ and $\xi_{sb}^D = 0$. If we restate these FC couplings to their nonzero value, the situation becomes even worse.

We obtain that, for $M_c = 200$ GeV, the model III contribution in this case is about a factor of 40 larger than the SM amplitude. When M_c increases to about 3–4 TeV the two contributions become comparable. Thus $B(B \rightarrow X_s \gamma)$ restricts

$$M_c \gtrsim 5 \text{ TeV} \qquad (48)$$

in this version of model III with the choice of couplings and masses needed to account for R_b^{expt}; see Eqs. (23) and (24). However, Eq. (48) is in striking conflict with the bound imposed by the ρ parameter [see Eq. (37)]. Moreover, we must remember that perturbation theory itself may start to have problems when scalar masses become so large.

In case 2, when the FC couplings are set to zero, we can reproduce the results of model II [19], whose compatibility with the present EW data is known to be still possible albeit in a small region of the parameter space. For nonzero FC couplings and when the couplings satisfy the conditions shown in Eq. (28), we can also get agreement at the 2σ level with the experimental constraint in Eq. (38). In this case, too, the ξ_{cc}^U and ξ_{ss}^D couplings are not relevant. The neutral scalar and pseudoscalar masses are required to lie in the narrow range specified by Eq. (24) and the charged scalar mass is supposed to satisfy both Eqs. (28) and (37), i.e.,

$$150 \text{ GeV} \lesssim M_c \lesssim 200 \text{ GeV}. \qquad (49)$$

Therefore, from our analysis of the constraints we can deduce that it is in general very difficult to accomodate the present value of R_b^{expt} in model III. However, if we assume that the FC couplings are arbitrary and dictated only by phenomenology, then, in principle, it is still possible to find a very small region of the parameter space in which model III

is compatible with the important experimental results. The values of the neutral scalar and pseudoscalar masses are required to fit the narrow window of Eq. (24) and are very close to their experimental lower bound. In order to increase them and still agree with R_b^{expt} we would need a heavier M_c and this would be in conflict with Eq. (49).

We recall that similar difficulties are present in model II as well [19]. However, the important difference with respect to model II is that the analysis of R_b and of the additional constraints on model III give us some hints on the possible range of the new FC couplings. These can then be used to explore interesting experimental consequences in FC transitions [7–10].

VI. REMARKS ON THE EXPERIMENTAL ASPECTS OF R_b AND R_c, R_{b+c}, AND R_l

The preceding discussion leads us to conclude that model III does not provide a *natural* explaination for the R_b *anomaly*. In particular, it requires the existence of neutral scalars and a pseudoscalar (h^0 and A^0) with very light masses as in Eq. (24) and of charged scalars in the range 150 GeV $\leq M_c \leq$ 200 GeV. The model may well be wrong and/or incomplete. We view the model as an illustration of the kind of theoretical scenarios that can result from a rather minimal extension of the SM, namely, due to the introduction of an extra Higgs doublet. The main virtue of the model is that it gives a reasonably well-defined theoretical framework in which experimental constraints on flavor-changing scalar couplings can be systematically categorized.

While the model may well be wrong, it is perhaps also of some use to question the experimental results, i.e., R_b^{expt} (and R_c^{expt}). As alluded to in the Introduction, the experimental analyses for R_b and R_c are correlated [1]. The deviation from the SM given in Eq. (2) appears quite significant ($\sim 3\sigma$), but this is only after the results from all the four LEP detectors and several different data sets are combined, including their systematic errors. One interesting aspect of the R_b results is that all the experiments find that $R_b^{\text{expt}} > R_b^{\text{SM}}$ although the significance of individual data sets is typically $\sim (1-2)\sigma$. The final errors given in Eq. (2) include statistical and systematic errors. To the extent that the experiments are truly independent, one is tempted to interpret that they confirm each other at least on this overall trend. On the other hand, it is also conceivable that this is a reflection of the fact that some of the systematics (shared by the experiments) are causing the problem.

Ironically R_b^{expt} and R_c^{expt} deviate oppositely from the SM values. In fact, using Ref. [1] we get

$$R_b^{\text{expt}} + R_c^{\text{expt}} = (0.2219 \pm 0.0017) + (0.1543 \pm 0.0074)$$
$$= 0.376 \pm 0.008, \tag{50}$$

which is quite consistent with the SM:

$$R_b^{\text{SM}} + R_c^{\text{SM}} = 0.388. \tag{51}$$

It is then natural to be concerned that the experimental effect could, in part, arise from misidentification of flavors.

Indeed we suggest a new observable R_{b+c}, defined as

$$R_{b+c} = \frac{\Gamma(Z \to b\bar{b} \text{ or } c\bar{c})}{\Gamma(Z \to \text{hadrons})}. \tag{52}$$

This is a very useful observable as it shares the theoretical cleanliness of R_b and R_c: it is insensitive to QCD corrections. It has significant experimental advantages, though, as separation between b and c (which is often difficult) need not be made. As a specific example, when charm or bottom decays semileptonically, the hardness of the lepton is often used to distinguish bottom from charm. With the use of R_{b+c}, one only needs to separate these heavy flavors from the really light ones (u,d,s).

Of course R_{b+c}^{expt} cannot be obtained by adding the existing numbers for R_b^{expt} and R_c^{expt} and we will have to await a separate experimental analysis for that. Meantime, we note that R_l, given by

$$R_l = \frac{\Gamma(Z \to \text{hadrons})}{\Gamma(Z \to l^+ l^-)}, \tag{53}$$

for which experimental numbers are available [1], does contain information on $\Gamma(Z \to b\bar{b} \text{ or } c\bar{c})$. Indeed [1],

$$R_l^{\text{expt}} = 20.788 \pm 0.032, \tag{54}$$

is rather precisely known with an accuracy of $\sim 0.15\%$ which is significantly better than R_b^{expt} (0.7%) or R_c^{expt} (4.5%). R_l, though, does depend on QCD corrections. The calculation of R_l is outlined in Appendix B.

It is important to observe that, to calculate the SM prediction (R_l^{SM}), we need to use $\alpha_s(M_Z)$ deduced from other physical methods [i.e., not $\Gamma(Z \to \text{hadrons})$]. In this way, R_l^{expt} can provide another constraint on any global fit of the SM. Two independent determinations of $\alpha_s(M_Z)$, for example, come from the lattice [32,20] and from the event shapes in $e^+ e^-$ annihilation [20]:

$$\alpha_s^{\text{latt}}(M_Z) = 0.110 \pm 0.006,$$

$$\alpha_s^{e^+ e^-}(M_Z) = 0.121 \pm 0.006. \tag{55}$$

We will use the average of the two: $\bar{\alpha}_s(M_Z) \simeq 0.116 \pm 0.006$. Using Table III in Appendix II, we then get the SM prediction

$$R_l^{\text{SM}} = 20.748 \pm 0.043. \tag{56}$$

The error in Eq. (56) corresponds to the 0.006 error (to 1σ) estimates on the central value of $\bar{\alpha}_s(M_Z)$. Comparing Eqs. (54) and (56), we see that R_l^{SM} is consistent with the experimental number, i.e., within about 1σ of the error on the experiment alone.

In passing we note that if the true $\alpha_s(M_Z)$ was taken to be 0.110, then

$$R_l[\alpha_s(M_Z) = 0.110] = 20.706, \tag{57}$$

which would start to deviate from the experimental result in Eq. (54) at the 2.6σ level. But with the current experimental accuracy, this deviation only occurs if one attributes essentially no error to the 0.110 central value of $\alpha_s(M_Z)$ [33]. We
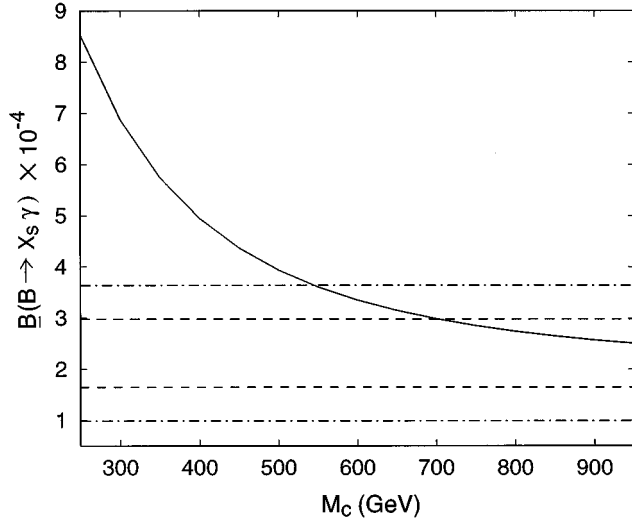
FIG. 2. $B(B \to X_s \gamma)$ in model III. The experimental result at 1σ (dashed line) and 2σ (dot-dashed line) is also given.

do not consider it reliable, at present, to reduce the theoretical errors so sharply. It is clearly important, though, that the efforts towards improved evaluations of $\alpha_s(M_Z)$ be continued, as then the experimental precision on R_l could be used more effectively to signal new physics.

VII. DISREGARDING R_B^{expt}

Given the previous analysis, we want now to reexamine model III without imposing the constraint coming from R_b^{expt}. Instead, we will give predictions for R_b, R_c, and R_{b+c} from the model, subjecting it only to the ρ parameter and $B(B \to X_s \gamma)$.

If we disregard R_b^{expt}, then there is no need to enhance the ξ_{bb}^D and ξ_{sb}^D couplings anymore. We will first consider the case in which all the λ_{ij} parameters in Eq. (16) are of order 1. In this way we can study the behavior of model III in a vast region of its parameter space. We will then comment about the different scenarios that are possible.

In the case in which all the λ_{ij} parameters of Eq. (16) are of order 1, model III predicts a $B(B \to X_s \gamma)$ compatible with experiments at the 2σ level, for $M_c \gtrsim 600$ GeV, as we can see in Fig. 2. As soon as ξ_{bb}^D is not enhanced anymore, the contribution of the neutral scalars and pseudoscalar is completely negligible. Therefore, both the value of the mixing angle α and of the neutral scalar and pseudoscalar masses (M_H, M_h, and M_A) are irrelevant. In particular, Fig. 2 is obtained for $\alpha = \pi/4$ and values for (M_H, M_h, M_A) resulting from the fit to $\Delta\rho_0$, as we will discuss in a while. Because of the qualitative character of our analysis, at this point it suffices to seek consistency with the experiment at the 2σ level. Indeed, we took as reference the SM calculation [31], which is already affected by a large uncertainty, and computed only the leading corrections due to the new scalar bosons of model III, i.e., without considering the complete leading order (LO) effective Hamiltonian analysis. From Fig. 2 we also note that, for $M_c \gtrsim 600$ GeV, model III is difficult to distinguish from the SM (again within 2σ), unless the
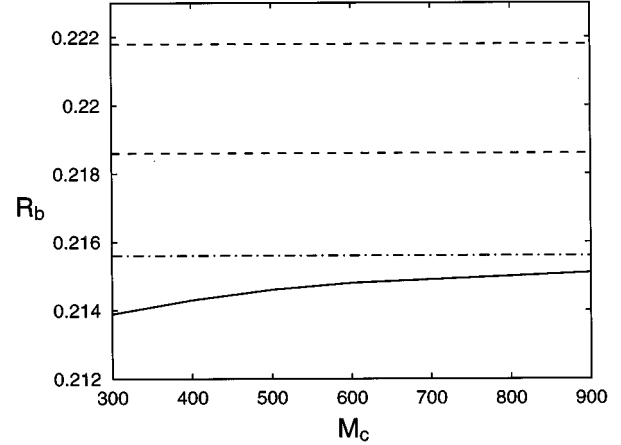

FIG. 3. R_b in model III with $\lambda_{ij} \sim 1$ (solid line) compared to the SM prediction $R_b^{\mathrm{SM}} = 0.2156$ (dot-dashed line). The experimental band (dashed line) is also given.

present SM calculation $[B(B \to X_s \gamma) = (1.9 \pm 0.6) \times 10^{-4}$ [31]] is improved [34].

With the requirement of a large M_c coming from $B(B \to X_s \gamma)$, we need to consider again the discussion of the ρ parameter and modify it accordingly. The charged scalar cannot be the heaviest scalar particle anymore, otherwise $\Delta\rho_0^{\mathrm{new}}$ would be as in Eq. (36) and would contradict the present global fit result [see Eq. (35)]. As already noted in Ref. [19] for model II, there are two other possible scenarios

$$M_H, M_h \lesssim M_c \lesssim M_A \quad \text{and} \quad M_A \lesssim M_c \lesssim M_H, M_h, \quad (58)$$

in which $\Delta\rho_0^{\mathrm{new}}$, as given by Eq. (33), turns out to be negative, and has in this way the extra advantage of canceling the effect of the top quark SM contribution [see Eq. (30)]. We note that none of the previous scenarios would give an enhanced value of R_b, because in that case M_A and M_h would be required to be equal and light (see Sec. III).

From a direct numerical evaluation of $\Delta\rho_0^{\mathrm{new}}$, we find that there may exist many possible sets of mass parameters for which Eq. (35) can be satisfied. For instance, let us consider
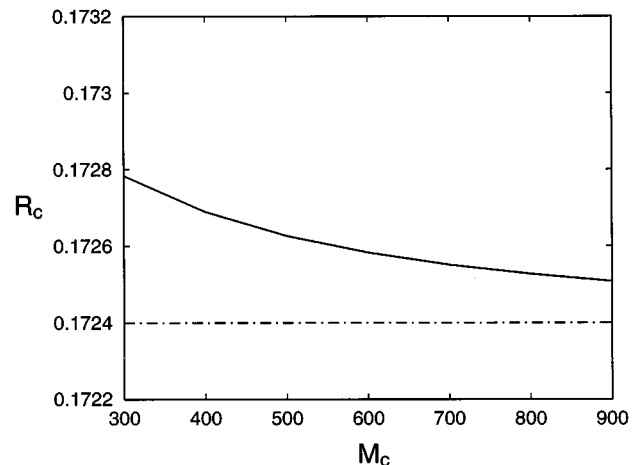

FIG. 4. R_c in model III with $\lambda_{ij} \sim 1$ (solid line) compared to the SM prediction $R_c^{\mathrm{SM}} = 0.1724$ (dot-dashed line).
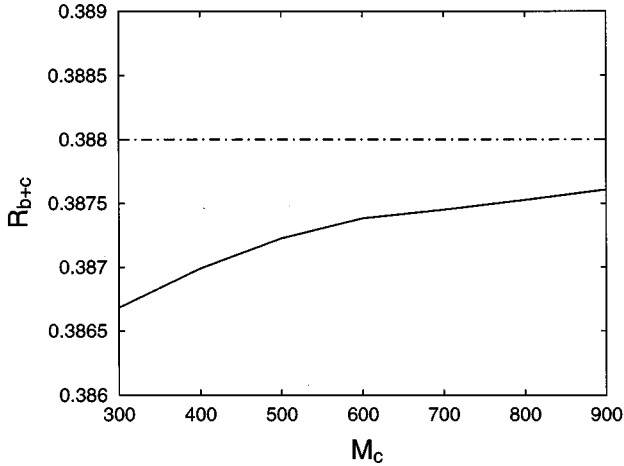
FIG. 5. R_{b+c} in model III with $\lambda_{ij} \sim 1$ (solid) compared to the SM prediction (dot-dashed line).

the case in which $M_H, M_h \lesssim M_c \lesssim M_A$. The other case in Eq. (58) has been studied too and it gives comparable results [39]. In order to have a small $\Delta \rho_0^{new}$, it is crucial that M_c and M_A be not too far apart. One possible optimal set of values for the mass parameters is given by the ratios $M_H = 0.4 M_c$, $M_h = 0.5 M_c$, and $M_A = 1.1 M_c$. In this case, the results for R_b, R_c, and R_{b+c} are illustrated in Figs. 3, 4, and 5 respectively. The SM predictions are also plotted for comparison. In the case of R_b we also plot the experimental result with its uncertainty (for $R_c = R_c^{SM}$). The experimental band is not shown in Fig. 4 as, for now, the experimental errors on R_c are very large. Clearly, in model III, R_b is less than R_b^{SM} and R_c is larger than R_c^{SM} on a very large region of the parameter space.

There may be a region of the parameter space, when both ξ_{tt}^U and ξ_{ct}^U are suppressed, in which the prediction of model III is almost identical to the SM one. In fact, the only large distinctive couplings for model III are the ξ_{ij}^U couplings, and if we suppress them, we make model III mimic the SM behavior. However, if the present experimental result persists, then just mimicking the SM is not enough. In this case model III will survive only in a small region of its parameter space, when the ξ_{ij}^D couplings are enhanced and the ξ_{ij}^U ones are suppressed (case 2 of Sec. III), as we discussed at length in Secs. III–V.

VIII. CONCLUSIONS

We analyzed the decays $Z \to b\bar{b}$ and $Z \to c\bar{c}$ in 2HDM's with FCSC's, often called model III. We find that R_b^{expt} places severe constraints on this model. There is only a very narrow window of the parameter space of the model in which this scenario can be reconciled with constraints from the ρ parameter and $B(B \to X_s \gamma)$: 50 GeV $\leqslant M_h \sim M_A < 70$ GeV and 150 GeV $\leqslant M_c \leqslant 200$ GeV, with significantly enhanced coupling of the neutral scalar and pseudoscalar to $b\bar{b}$ (and $b\bar{s}$) as in Eq. (28).

Since aspects of the experimental analysis are of some concern, we also examined the model by disregarding R_b^{expt} and we give the predictions for R_b, R_c, and R_{b+c} in this case. In particular, we find that, if the current trend of $R_b^{expt} > R_b^{SM}$ persists, then this class of models can only survive in a small region of the parameter space.

We also made the following points.

We emphasized the importance of R_l. To use its experimental cleanliness and precision more effectively, improvements in the theoretical determination of α_s are urged.

We suggested a new observable R_{b+c}. It is theoretically as clean as R_b and R_c but it should be more readily accessible experimentally.

In view of the fact that in models with FCSC's the rate for $Z \to c\bar{c}$ receives a correction which grows with m_t^2, we stressed that precise measurements of $Z \to c\bar{c}$ could provide unique constraints on the crucial tc vertex. Therefore we suggested an improved determination of $Z \to c\bar{c}$.

APPENDIX A: FEYNMAN RULES FOR MODEL III

In this appendix we summarize the Feynman rules for model III which are used in many of the calculations presented in the paper.

1. Fermion-scalar couplings

We present the Feynman rules for the couplings of the scalar fields H^1 (neutral scalar), H^2 (neutral pseudoscalar), and H^+ (charged scalar), to up-type and down-type quarks, as can be derived from the Yukawa Lagrangian of model III [Eqs. (8)–(13)]. Following the discussion of Sec. II, these are the Feynman rules we need in our calculation of R_b.

$$\frac{-i}{2\sqrt{2}} \left((\xi_{ij}^{U,D} + \xi_{ij}^{U,D*}) + (\xi_{ij}^{U,D} - \xi_{ij}^{U,D*})\gamma_5 \right)$$

$$\frac{1}{2\sqrt{2}} \left((\xi_{ij}^{U,D} - \xi_{ij}^{U,D*}) + (\xi_{ij}^{U,D} + \xi_{ij}^{U,D*})\gamma_5 \right)$$

$$\frac{-i}{2} \left(V_{CKM} \cdot \xi_{ij}^D (1 + \gamma_5) - \xi_{ij}^U \cdot V_{CKM}(1 - \gamma_5) \right)$$

Although the $\xi_{ij}^{U,D}$ couplings are left complex in the above, in practice, in our calculation we assumed they are real, i.e., $\xi_{ij}^{U,D} \simeq \xi_{ij}^{U,D*}$ as we were not concerned with any phase-dependent effects.

2. Gauge boson−scalar couplings

Here is a list of the Z- and W-boson interactions with model III scalar fields, useful for the computation of $\Delta\rho_0^{\text{new}}$. We report them in terms of scalar mass eigenstates $\overline{H}^0$, h^0, A^0, and H^+ in order to make contact with the discussion given in Sec. IV and with the literature [23,14]. We always have to remember the relations [see Eqs. (11) and (12)] between the scalar mass eigenstates and (H^0, H^1, H^2, H^+) and use the fact that neither ZH^0H^1 nor ZH^0H^2 couplings are present [23,14].

APPENDIX B: CALCULATION OF R_l AS A FUNCTION OF α_s

In this appendix we will use the value of $\alpha_s(M_Z)$ deduced from physics other than the width for $Z\rightarrow$hadrons to predict $\Gamma^{\text{SM}}(Z\rightarrow$hadrons) and R_l^{SM} to $O(\alpha_s^2)$. Mostly, we follow Bernabéu *et al.* [2], who give expressions for various corrections to $\Gamma(Z\rightarrow f\bar{f})$, for both quarks and leptons.

Let us rewrite the expression for the width of $Z\rightarrow f\bar{f}$ as

$$\Gamma(Z\rightarrow f\bar{f}) = \Gamma_0^f(1+\Delta_{\text{EW}}^f)(1+\Delta_{\text{QCD}}^f), \quad (\text{B1})$$

where Γ_0^f is the tree-level expression, in which some effects of the EW corrections have been reabsorbed in the renormal-

TABLE I. Values of Δ_{EW}^f, for different flavors, in units of (10^{-3}). They have been evaluated for $m_t=176$ GeV and $m_H=200$ GeV.

ν	e,μ,τ	u,c	d,s	b
3.739	2.736	2.200	2.778	-13.848

ization of the couplings (see conventions adopted in [2]). Δ_{EW}^f includes only corrections which do not depend on α_s, i.e., pure EW corrections and QED corrections. They are presented in detail in Ref. [2] [Eqs. (9), (15), and (17); see also references therein] and we will not discuss them here. We give their numerical values [35] in Table I. Δ_{QCD}^f represents mostly α_s-dependent corrections which can be subdivided as

$$\Delta_{\text{QCD}}^f = \delta_{\text{QCD}} + \delta_{\mu\text{QCD}}^f + \delta_{t\text{QCD}}^f. \quad (\text{B2})$$

We briefly discuss each of them below.

The strong corrections to the basic V,A vertex ($V=\gamma^\mu$, $A=\gamma^\mu\gamma^5$) are flavor independent and at $O(\alpha_s^2)$ are given by

$$\delta_{\text{QCD}} = \frac{\alpha_s(M_Z)}{\pi} + 1.41\left(\frac{\alpha_s(M_Z)}{\pi}\right)^2. \quad (\text{B3})$$

This is the dominant effect amounting to about 3–4 % (see Table II).

$\delta_{\mu\text{QCD}}^f$ represents corrections due to kinematic effects of external masses, including mass-dependent QCD corrections [36,37]. We decide to include in the same factor also non-QCD mass-dependent corrections to the axial vector couplings, in order to make the presentation more compact. Strictly speaking, this correction should be included in Δ_{EW}^f. Based on the results given in Refs. [36,37], we deduce [38]

$$\delta_{\mu\text{QCD}}^f = \frac{3\mu_f^2}{v_f^2+a_f^2}\left[-\frac{1}{2}a_f^2\left(1+\frac{11}{3}\frac{\alpha_s}{\pi}\right)+v_f^2\left(\frac{\alpha_s}{\pi}\right)\right], \quad (\text{B4})$$

where $\mu_f^2 = 4\overline{m}_f^2(M_Z)/m_Z^2$, $\overline{m}_f(M_Z)$ being the running mass at the Z scale, and

$$v_e = -1+4x_W, \quad a_e = +1, \quad v_u = +1-\frac{8}{3}x_W,$$

$$a_u = -1, \quad v_d = -1+\frac{4}{3}x_W, \quad a_d = +1. \quad (\text{B5})$$

TABLE II. Values of different QCD corrections (in units of 10^{-3}), for different values of $\alpha_s(M_Z)$.

$\alpha_s(M_Z)$	δ_{QCD}	$\delta_{\mu\text{QCD}}^b$	$\delta_{\mu\text{QCD}}^c$	$\delta_{t\text{QCD}}^u$	$\delta_{t\text{QCD}}^d$
0.105	34.998	−5.417	−0.560	4.260	−3.305
0.110	36.742	−5.179	−0.514	4.676	−3.628
0.115	38.495	−4.938	−0.467	5.111	−3.965
0.120	40.254	−4.695	−0.420	5.565	−4.317
0.125	42.021	−4.450	−0.372	6.038	−4.684

Using Eq. (2) from Ref. [2], we obtain $x_W = 0.2314$ (where $x_W = \sin^2\theta_W$). Numerically, $\delta^b_{\mu\mathrm{QCD}} \simeq -5 \times 10^{-3}$ and $\delta^c_{\mu\mathrm{QCD}} \sim -0.5 \times 10^{-3}$ (see Table II for their α_s dependence). This kind of correction is also relevant, without $O(\alpha_s)$ terms, for the τ lepton, in which case it amounts to $\delta^\tau_\mu \simeq -2 \times 10^{-3}$.

At $O(\alpha_s^2)$ the large mass splitting between the t and b quarks gives rise to a correction $\delta^f_{t\mathrm{QCD}}$ due to triangular quark loops affecting the axial vector current [37]:

$$\delta^f_{t\mathrm{QCD}} = -\frac{a_t a_f}{v_f^2 + a_f^2}\left(\frac{\alpha_s}{\pi}\right)^2 f(\mu_t), \qquad (\mathrm{B6})$$

where $f(\mu_t)$ can be written as [37,2]

$$f(\mu_t) = \ln\frac{4}{\mu_t^2} - 3.083 + 0.346\frac{1}{\mu_t^2} + 0.211\frac{1}{\mu_t^4}. \qquad (\mathrm{B7})$$

For $m_t = 176$ GeV we use $f(\mu_t) = -4.374$. Thus, this correction effects $+2/3$-charge quarks positively and $-1/3$-charge quarks negatively and for each flavor it is about 0.4–0.5 %, as we can read from Table II.

Having identified all the corrections to $\Gamma_f = \Gamma(Z \to f\bar{f})$, for both quarks and leptons, we then consider R_l and define

$$R_l = \frac{(\Gamma_u + \Gamma_d + \Gamma_s + \Gamma_c + \Gamma_b)}{\Gamma_l}$$

$$= \sum_{f=u,d,s,c,b} R^f_{l,0} \frac{(1 + \Delta^f_{\mathrm{EW}})}{(1 + \Delta^l_{\mathrm{EW}} + \delta^\tau_\mu/3)}(1 + \Delta^f_{\mathrm{QCD}}), \quad (\mathrm{B8})$$

where $\Gamma_l = (\Gamma_e + \Gamma_\mu + \Gamma_\tau)/3$ and Δ^l_{EW} represents the EW corrections common to all the lepton species (see Table I). We have denoted by $R^f_{l,0}$ the tree-level ratios for each quark species. They are given by

TABLE III. Values of R_l and its QCD corrections (in units of 10^{-3}) as functions of $\alpha_s(M_Z)$.

$\alpha_s(M_Z)$	Δ^u_{QCD}	Δ^c_{QCD}	$\Delta^{d,s}_{\mathrm{QCD}}$	Δ^b_{QCD}	R_l
0.105	39.258	38.698	31.693	26.276	20.6715
0.110	41.418	40.904	33.114	27.935	20.7060
0.115	43.606	43.139	34.530	29.592	20.7410
0.120	45.819	45.399	35.937	31.242	20.7759
0.125	48.059	47.678	37.337	32.887	20.8108

$$R^u_{l,0} = \frac{\Gamma^u_0}{\Gamma^e_0} = 3\frac{v_u^2 + a_u^2}{v_e^2 + a_e^2},$$

$$R^d_{l,0} = \frac{\Gamma^d_0}{\Gamma^e_0} = 3\frac{v_d^2 + a_d^2}{v_e^2 + a_e^2}, \qquad (\mathrm{B9})$$

and for $x_W = 0.2348$ they can be estimated to be $R^u_{l,0} = 3.4209$ and $R^d_{l,0} = 4.4101$.

Finally, Δ^f_{QCD} represents the total QCD corrections for each flavor. They are deduced from the previous discussion and their numerical values are summarized in Table III, together with R_l, for different values of $\alpha_s(M_Z)$.

Using the values for Δ^f_{EW} given, for each flavor, in Table I, R_l can be parametrized as $[\alpha_s = \alpha_s(M_Z)]$

$$R_l = R^u_{l,0}(1.000\,219)[2 + \Delta^u_{\mathrm{QCD}}(\alpha_s) + \Delta^c_{\mathrm{QCD}}(\alpha_s)]$$
$$+ 2R^d_{l,0}(1.000\,796)[1 + \Delta^{d,s}_{\mathrm{QCD}}(\alpha_s)]$$
$$+ R^d_{l,0}(0.984\,199)[1 + \Delta^b_{\mathrm{QCD}}(\alpha_s)], \qquad (\mathrm{B10})$$

from which we deduce the values reported in Table III.

[1] *Proceedings of the International Europhysics Conference on High Energy Physics*, Brussels, 1995 (World Scientific, Singapore, 1996); 17th International Symposium on Lepton-Photon Interactions, Beijing, China, 1995 (unpublished). See also LEP Electroweak Working Group Report 95-02 (unpublished).

[2] J. Bernabéu, A. Pich, and A. Santamaria, Nucl. Phys. **B363**, 326 (1991).

[3] Here is an illustrative sample of some of the existing studies: A. Denner, R.J. Guth, W. Hollik, and J.H. Kühn, Z. Phys. C **51**, 695 (1991); A.K. Grant, Phys. Rev. D **51**, 207 (1995); J.T. Liu and D. Ng, Phys. Lett. B **342**, 262 (1995); E. Ma and D. Ng, Phys. Rev. D **53**, 255 (1996); J.D. Wells, C. Kolda, and G.L. Kane, Phys. Lett. B **338**, 219 (1994); J.D. Wells and G.L. Kane, Phys. Rev. Lett. **76**, 869 (1996); G. Bhattacharyya, G. Branco, and W.-S. Hou, Phys. Rev. D **54**, 2114 (1996); T. Rizzo, presented at the Heavy Flavor Symposium, Haifa, Israel, 1995 (unpublished); P. Chiappetta, J. Layssac, F.M. Renard, and C. Verzegnassi, Phys. Rev. D **54**, 789 (1996); G. Altarelli, N. di Bartolomeo, F. Feruglio, R. Gatto, and M.L. Mangano, Phys. Lett. B 375, 292 (1996); P. Bamert, C.P.

Burgess, J.M. Cline, D. London and E. Nardi, Phys. Rev. D (to be published).

[4] T.P. Cheng and M. Sher, Phys. Rev. D **35**, 3484 (1987); M. Sher and Y. Yuan, *ibid.* **44**, 1461 (1991); see also Ref. [5].

[5] A. Antaramian, L.J. Hall, and A. Rasin, Phys. Rev. Lett. **69**, 1871 (1992).

[6] L.J. Hall and S. Weinberg, Phys. Rev. D **48**, R979 (1993).

[7] W.S. Hou, Phys. Lett. B **296**, 179 (1992); D. Chang, W.S. Hou, and W.Y. Keung, Phys. Rev. D **48**, 217 (1993).

[8] M. Luke and M.J. Savage, Phys. Lett. B **307**, 387 (1993); M.J. Savage, *ibid.* **266**, 135 (1991).

[9] D. Atwood, L. Reina, and A. Soni, Phys. Rev. D **53**, R1199 (1996).

[10] D. Atwood, L. Reina, and A. Soni, Phys. Rev. Lett. **75**, 3800 (1995).

[11] S. Glashow and S. Weinberg, Phys. Rev. D **15**, 1958 (1977).

[12] For a review see J. Gunion, H. Haber, G. Kane, and S. Dawson, *The Higgs Hunter's Guide* (Addison-Wesley, New York, 1990).

[13] T. Han, R.D. Peccei, and X. Zhang, Nucl. Phys. **B454**, 527 (1995).

[14] C.D. Froggatt, R.G. Moorhouse, and I.G. Knowles, Nucl. Phys. **B386**, 63 (1992).

[15] A detailed phenomenological analysis [16] shows that for the first family one needs $\lambda_{ij} \simeq 0.1$ in Eq. (16) in order to satisfy the bounds from K^0-$\bar{K}^0$ and B^0-$\bar{B}^0$ mixing over a large region of the parameter space of model III. Therefore, in this work we will assume that the FC couplings which involve the first family are negligibly small.

[16] D. Atwood, L. Reina, and A. Soni, Report No. JL-TH-96-15 (unpublished).

[17] In our calculation all the quarks except the top quark are taken to be massless, keeping $m_q \neq 0$ only in the $\xi_{ij}^{U,D}$ couplings as in Eq. (16) and in the determination of some corrections to R_l, when they become relevant to the degree of accuracy that we seek.

[18] A. Denner, R.J. Guth, W. Hollik, and J.H. Kühn, Z. Phys. C **51**, 695 (1991).

[19] A.K. Grant, Phys. Rev. D **51**, 207 (1995).

[20] Particle Data Group, L. Montanet *et al.*, Phys. Rev. D **50**, 1173 (1994).

[21] In obtaining our results for R_b we had calculated both $Z \to b\bar{b}$ and $Z \to c\bar{c}$ in model III. Therefore the corresponding experimental number differs a little bit from that in Eq. (2) which is determined by holding R_c fixed to its experimental value (see Ref. [1]).

[22] P. Langacker, in *Precision Tests of the Standard Electroweak Model*, edited by P. Langacker (World Scientific, Singapore, 1994).

[23] S. Bertolini, Nucl. Phys. **B272**, 77 (1986).

[24] CDF Collaboration, F. Abe *et al.*, Phys. Rev. Lett. **74**, 2626 (1995); D0 Collaboration, S. Abachi *et al.*, *ibid.* **74**, 2632 (1995).

[25] CLEO Collaboration, R. Ammar *et al.*, Phys. Rev. Lett. **71**, 674 (1993); CLEO Collaboration, M.S. Alam *et al.*, *ibid.* **74**, 2885 (1995).

[26] Note that we are considering the case $\alpha = 0$, as required by the best fit of R_b.

[27] B. Grinstein, R. Springer, and M. Wise, Phys. Lett. B **202**, 132 (1988); Nucl. Phys. **B339**, 269 (1990); R. Grigjanis, P.J. O'Donnel, M. Sutherland, and H. Navelet, Phys. Lett. B **213**, 355 (1988); **223**, 239 (1989); **237**, 252 (1990); G. Cella, G. Curci, G. Ricciardi, and A. Viceré, *ibid.* **248**, 181 (1990); **325**, 227 (1994); M. Misiak, Nucl. Phys. **B393**, 23 (1993); K. Adel and Y.P. Yao, Phys. Rev. D **49**, 4945 (1994).

[28] M. Ciuchini, E. Franco, G. Martinelli, L. Reina, and L. Silvestrini, Phys. Lett. B **316**, 127 (1993); Nucl. Phys. **B421**, 41 (1994).

[29] A.J. Buras, M. Misiak, M. Münz, and S. Pokorski, Nucl. Phys. **B424**, 137 (1994).

[30] We use the same normalization as in Ref. [29], in order to check our result against the discussion of the problem in model II, as given in that paper.

[31] M. Ciuchini, E. Franco, G. Martinelli, L. Reina, and L. Silvestrini, Phys. Lett. B **344**, 137 (1994).

[32] A.X. El-Khadra, G. Hockney, A. Kronfeld, and P. Mackenzie, Phys. Rev. Lett. **69**, 729 (1992); C.T.H. Davies, K. Hornbostel, G.P. Lepage, A. Lidsey, J. Shigemitsu, and J. Sloan, Phys. Lett. B **345**, 42 (1995).

[33] In this regard see the analysis by M. Shifman [Report No. hep-ph/9511469 (unpublished)], using the Z-line shape (rather than R_l) and the value of α_s advocated by, M. Voloshin, Int. J. Mod. Phys. A **10**, 2865 (1995). It is interesting that both these observables (Z-line shape and R_l) lead to similar conclusions when $\alpha_s(M_Z) = 0.110$ is used.

[34] The theoretical prediction of $B(B \to X_s \gamma)$ from Ref. [31] includes some next-to-leading order (NLO) QCD corrections and the result could change in the future by a complete NLO analysis. We could have used in our analysis the fully consistent LO result for $B(B \to X_s \gamma)$, which is a little higher (see Refs. [31,29]), but this would not modify the qualitative results that we are giving.

[35] Δ_{EW}^f depends very weakly on m_H. The numerical values quoted in Table I are for $m_H = 200$ GeV.

[36] K.G. Chetyrkin and J.H. Kühn, Phys. Lett. B **248**, 359 (1990).

[37] B.A. Kniehl and J.H. Kühn, Nucl. Phys. **B329**, 547 (1990).

[38] Note that our Eq. (B4) differs from Eq. (19) of Ref. [2]. We derive Eq. (B4) from Ref. [36], where the results of Ref. [37] are improved by absorbing large $\ln M_Z^2/m_b^2$ through the use of the running mass $\bar{m}_b(M_Z)$. Using Eqs. (2) and (4) of Ref. [36] and substituting the on-shell mass m_b with the $\overline{MS}$ mass as in Eq. (9) therein, we confirm their result in Eq. (14). Thus we arrive at our Eq. (B4).

[39] When the ξ^D-type couplings are not enhanced and the scalar masses lie in the ranges given in Eq. (58), the leading contribution come from the charged scalar diagrams. Therefore the dependence on the phase α is irrelevant and our results will be given in particular for $\alpha = \pi/4$.